Minimum Mean-Square Error Resampling for Remotely Sensed Imagery

Gregory W. Wornell, David S. Kauffman, Bruce Sharpe

MacDonald Dettwiler & Associates Ltd.
13800 Commerce Parkway, Richmond, B.C.
Canada V6V 2J3

Abstract

Two families of optimum realizable resampling kernels are developed for use with remotely-sensed data in clean and noisy environments. These robust, model-based kernels are designed for minimum mean-square resampling error.

The first family of kernels is designed for use with Nyquist-sampled imagery. The resulting kernels offer performance as good as the best of the popular resamplers in clean environments, and superior performance in noisy environments.

The second family of kernels is designed for resampling aliased imagery. For smaller kernels, resampling performance improvement is achieved over traditional resamplers. Most notably, experiments show that the 4×4-point kernel can reduce resampling error by more than 22% over cubic convolution.

Introduction

The need for radiometrically-accurate resampling algorithms arises regularly in problems of quantitative remote sensing. Indeed, resampling plays a crucial role in the correction of raw satellite image data and its and transformation to a UTM coordinate grid.

In general, the problem of resampling or interpolation involves the reconstruction of a waveform known only at a finite collection of points—usually on a regular sampling grid. Most interpolators currently in use fall into two categories:

Spline-based Interpolation Here, the sampled data is splined together with curves of the desired form. Nearest-neighbour, bilinear, and cubic-convolution interpolation are examples of this method [3], corresponding, respectively, to piecewise-constant, linear, and cubic-polynomial splines.

Sinc-based Interpolation Here it is assumed that the waveform to be reconstructed is band-limited and that the sampling grid is sufficiently dense. In this case, optimum interpolation requires the use of sinc functions and is, in fact, *unrealizable*. Realizable approximations to this method have relied on the use of windowing techniques [4] [3].

Inherently, both approaches make use of certain smoothness assumptions about the waveform being reconstructed[1]. And, while the resulting interpolators have been shown empirically effective—both subjectively and in terms of RMS error—they have not been designed to be optimal in any particular sense.

In this work, we describe a framework in which to design families of optimum realizable resampling kernels which give minimum mean-square resampling error based on some simple but reasonable models for the underlying imagery. Some related formulations have been considered in [1] [2].

A Framework

Through the remote sensing process, distorted and corrupted samples of the ground radiance image constitute the available raw data. While various effects such as Earth curvature and satellite motion cause these samples to be irregularly spaced, we shall assume that the sampling falls approximately on a rectangular lattice at some rotation.

It will also be convenient to employ imagery models with a degree of statistical *separability* with respect to the along-scan and across-scan directions. While this assumption has no strong physical basis, it ensures that we obtain separable resampling kernels suitable for two-pass processing, and it allows us to consider along-scan and across-scan resampling as two separate one-dimensional problems.

In its discrete form, the general one-dimensional resampling environment is as shown in Fig. 1. The continuous-time signal $x(t)$ represents the radiance of ground imagery. The linear shift-invariant filter $g(t)$ models the sensor distortions before and during sampling. With Landsat data, for example, $g(t)$ can be used to account for detector size effects (cross-scan) and band-pass filtering (along-scan) in the sensor as well as non-ideal sampling. The additive sequence $w[n]$ models noise in the acquisition process arising during sensing, sampling at rate T, and quantization. The available data for resampling is then $v[n]$.

The resampler is represented by the filter $\hat{h}[n]$. To ensure that this filter is realizable and stable, we enforce the constraint that $\hat{h}[n]$ have finite extent, i.e.,

$$\hat{h}[n] = 0, \; n < M, \; n > N. \tag{1}$$

for some $M < N$ (usually $M = -N + 1$).

Finally, we want the resampler output at some instant n_0 to best recover $x(t_0)$ for an arbitrary t_0 from the sequence $v[n]$, though we recognize that during subsequent stages of processing we may ultimately be interested in recovering $x(t_0)$.

[1] Indeed, without some additional information there is no "correct" way to reconstruct the waveform.

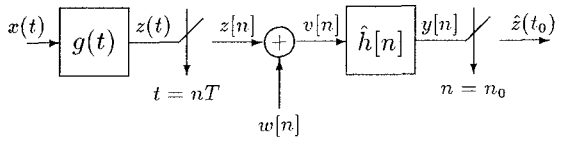

Figure 1: The general resampling environment.

We shall assume that $x(t)$ is a zero-mean, wide-sense stationary random process. The zero-mean assumption is not serious, for we may always process our non-zero mean imagery by removing the mean prior to resampling and restoring it immediately thereafter. The wide-sense stationarity assumption is somewhat stronger, but results in resampling kernels which are invariant over the imagery. As a consequence of stationarity, we may write the autocorrelation of $x(t)$ as

$$R_x(\tau) = E[x(t)x(t-\tau)] \tag{2}$$

The noise sequence $w[n]$ is considered to be zero-mean and white with power σ^2, so that

$$R_w[k] = E[w[n]w[n-k]] = \begin{cases} \sigma^2 & k = 0 \\ 0 & k \neq 0 \end{cases} \tag{3}$$

Kernels for Band-limited Imagery

In this section, we assume that $x(t)$ is strictly band-limited and that the corresponding $z(t)$ has been sampled at or above the Nyquist-rate. Provided the sampling is noise-free ($\sigma^2 = 0$) it is well-known that $z(t_0)$ may be recovered, in principle, from the samples

$$v[n] = z[n] = z(nT), \; n = 0, \pm 1, \pm 2, \ldots \tag{4}$$

In particular, choosing a suitable $\alpha \in [0, 1)$ and integer n_0 such that

$$t_0 = (n_0 + \alpha)T, \tag{5}$$

Whittaker-Shannon sampling theory assures us that

$$z(t_0) = (h * z)[n_0] \tag{6}$$

where

$$h[n] = \operatorname{sinc}(n + \alpha) = \frac{\sin \pi(n+\alpha)}{\pi(n+\alpha)}. \tag{7}$$

Unfortunately, this sinc filter, corresponding to band-limited interpolation, has infinite extent and is, in fact, unrealizable. Moreover, we have only a finite segment of the sample sequence $z[n]$ available. While the truncated sinc filter seems a natural candidate for our resampling kernel, we shall see that, in fact, it is optimal only for a rather specific and atypical scenario.

Using a Wiener filtering framework, we may define our objective as minimizing the mean-square resampling error

$$\varepsilon = E\left[(z(t_0) - \hat{z}(t_0))^2\right] \tag{8}$$

where $\hat{z}(t_0)$ is the output of filter $\hat{h}[n]$ at n_0, *viz.*,

$$\hat{z}(t_0) = y[n_0] = \sum_{k=M}^{N} \hat{h}[k](z[n_0 - k] + w[n_0 - k]). \tag{9}$$

Note that we may express $z(t_0)$ in terms of the ideal interpolator $h[n]$ by

$$z(t_0) = \sum_{k=\infty}^{\infty} h[k]z[n_0 - k]. \tag{10}$$

By minimizing (8) using (9) and (10), it is straightforward to show that the optimal resampler $\hat{h}[n]$ satisfies the Toeplitz *normal* equations

$$\sum_{k=M}^{N} \hat{h}[k]R_z[n-k] + \hat{h}[n]\sigma^2 = \sum_{k=-\infty}^{\infty} h[k]R_z[n-k] \tag{11}$$

for $n = M, M+1, \ldots, N$.

If the samples $z[n]$ are modeled as a first-order autoregressive [AR(1)] sequence, then

$$R_z[k] \propto \rho^{|k|} \tag{12}$$

for some $|\rho| < 1$. These are popular simplified models for image processing. Note that ρ is a measure of the degree of correlation in the data, with $\rho = 0$ corresponding to white (uncorrelated) data. Empirical studies have shown that, for a variety of imagery, values of ρ near 1 are most applicable.

Using the AR(1) model, the normal equations may be solved to give the optimum resampler

$$\hat{h}[n] = \begin{cases} \sum_{k=0}^{\infty} h[-k+M]\rho^k & n = M \\ h[n] & M < n < N \\ \sum_{k=0}^{\infty} h[k+N]\rho^k & n = N \end{cases} \tag{13}$$

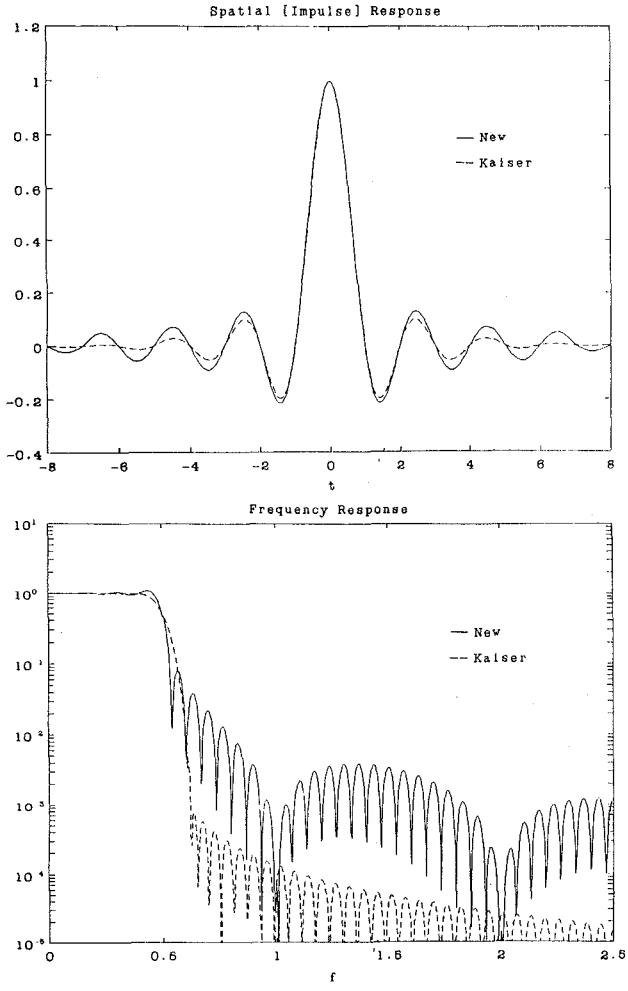

Figure 2: Spatial and frequency response characteristics of the optimal 16×16-point interpolator for band-limited imagery corresponding to $\rho \sim 1$ and $\sigma^2 = 0$. The Kaiser-windowed sinc interpolator is shown for comparison.

Evidently, this resampler is a generalization of the truncated-sinc filter, for when $\rho = 0$, $\hat{h}[n]$ is indeed a truncated sinc. However, for ρ near 1, $\hat{h}[n]$ is a truncated sinc whose end-points are reduced in magnitude. Note that in the limiting case $\rho \to 1$, the filter is normalized

$$\sum_{n=M}^{N} \hat{h}[n] = \sum_{k=-\infty}^{\infty} h[n] = 1, \tag{14}$$

obviating the need for mean-removal in the resampling process. Fig. 2 compares the spatial and frequency characteristics of the 16×16-point interpolator corresponding to $\rho \sim 1$ and $\sigma^2 = 0$ with that of the Kaiser-windowed sinc interpolator.

Kernel			Noise	Error (DN)	
Type	ρ	size	SNR	RMS	Peak
New	~ 1	2×2	–	4.9	25
Bilinear	–	2×2	–	5.1	26
New	~ 1	4×4	–	3.8	17
Cubic	–	4×4	–	3.2	15
New	~ 1	8×8	–	2.0	11
Hamming	–	8×8	–	1.8	8
New	~ 1	16×16	–	1.6	8
Kaiser	–	16×16	–	1.4	7
New	0.9	16×16	1 dB	16.5	75
Kaiser	–	16×16	1 dB	27.0	95
New	0.9	16×16	11 dB	7.4	36
Kaiser	–	16×16	11 dB	8.8	36

Table 1: Resampling performance of kernels for band-limited imagery.

Resampling Experiments

To evaluate the resampling kernels derived in this section, a 128×128-pixel test chip was twice resampled by one-half pixel both horizontally and vertically, and compared to a displaced version of the original chip. In some tests, the chip was artificially degraded by additive white Gaussian noise to achieve a prescribed signal-to-noise ratio (SNR) prior to resampling. As appropriate, comparisons are made to the traditional resampling schemes: bilinear interpolation, cubic convolution, Hamming-windowed sinc interpolation, and Kaiser-windowed ($\beta = 6$) sinc interpolation. As the results in Table 1 indicate, the new kernels are competitive with the best of the traditional resamplers in noise-free environments despite a markedly different kernel shape. Moreover, in the presence of noise, the new kernels offer much improved performance.

Kernels for Aliased Imagery

In the last section, it was assumed that $x(t)$ was band-limited. Unfortunately, in practice, imagery is only approximately band-limited and, in any case, is always sampled in a manner which introduces some aliasing. In this section, we develop an alternative set of kernels based upon a model which accounts for aliasing introduced in the sensing process.

We begin by modeling $x(t)$ as a continuous AR(1) process, for which the autocorrelation function satisfies

$$R(\tau) = E\left[x(t)x(t-\tau)\right] \propto e^{-\omega_0|\tau|} \tag{15}$$

where $\omega_0 > 0$ is a parameter. The choice of ω_0 specifies the degree of correlation in the data, and values near 0 are appropriate for imagery. Since the power spectrum for this process is

$$S_x(\omega) = \mathcal{F}\{R_x(\tau)\} \propto \frac{1}{1 + (\omega/\omega_0)^2}, \tag{16}$$

it is evident that $x(t)$ is, indeed, not band-limited. Note, also, that for some $0 < \rho < 1$, (15) may be re-written as

$$R(\tau) \propto \rho^{|\tau|/T} \tag{17}$$

where, evidently, $\omega_0 \approx 0$ corresponds to $\rho \approx 1$.

Now for arbitrary $R_z(\tau)$, the minimization of (8) subject to (9) gives the optimal resampler as the solution to the normal equations

$$\sum_{k=M}^{N} \hat{h}[k]R_z((n-k)T) + \sigma^2\hat{h}[n] = R_z((n+\alpha)T) \tag{18}$$

for $n = M, M+1, \ldots, N$.

In the absence of $g(t)$, this optimum resampler is given by

$$\hat{h}[n] = \begin{cases} (\rho^{-1(1-\alpha)} - \rho^{(1-\alpha)})/(\rho^{-1} - \rho) & n = 0 \\ (\rho^{-\alpha} - \rho^{\alpha})/(\rho^{-1} - \rho) & n = 1 \\ 0 & \text{otherwise} \end{cases} \tag{19}$$

which gives bilinear interpolation in the limit $\rho \to 1$. This rather surprising result, also deduced by Polydoros and Protonotarios [2], establishes that for such highly-correlated signals a two-point resampler is optimal. In fact, this is a consequence of the extensive aliasing in the samples of these signals.

More realistically, some low-pass filtering takes place in the sensor. In fact, if the sensor performs *natural* sampling, so that $g(t)$ is given by

$$g(t) = \begin{cases} 1/T & |t| < T/2 \\ 0 & |t| \geq T/2 \end{cases}, \tag{20}$$

then

$$R_z(\gamma T) = \begin{cases} \left[\rho^{1+|\gamma|} - 2\rho^{|\gamma|} + \rho^{1-|\gamma|} + 2(|\gamma|-1)\mu\right]/\mu^2 & |\gamma| \leq 1 \\ \left[\rho^{|\gamma|+1} - 2\rho^{|\gamma|} + \rho^{|\gamma|-1}\right]/\mu^2 & |\gamma| > 1 \end{cases} \tag{21}$$

where

$$\mu = \ln|\rho|. \tag{22}$$

Using this expression for $R_z(\cdot)$, the normal equations (18) may be solved numerically to obtain resamplers parameterized by ρ and σ^2. In noise-free environments ($\sigma^2 = 0$), these resamplers have a damped-sinc appearance similar to be that of the Kaiser-windowed sinc interpolators, but with stronger damping. Fig. 3 compares the spatial and frequency characteristics of the 4×4-point interpolator corresponding to $\rho = 0.9$ and $\sigma^2 = 0$ with those of cubic convolution.

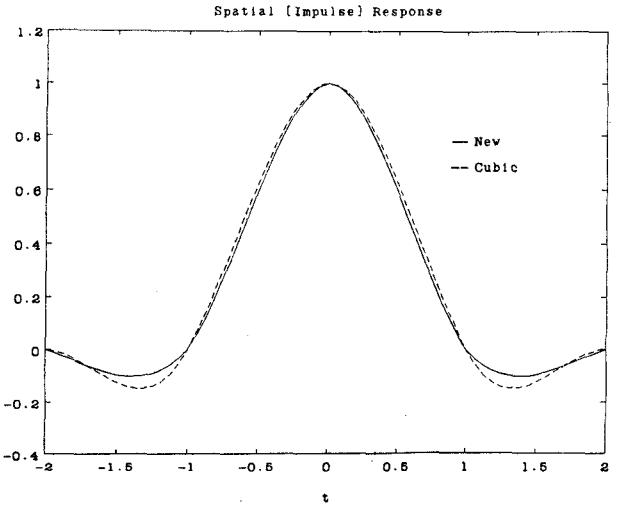

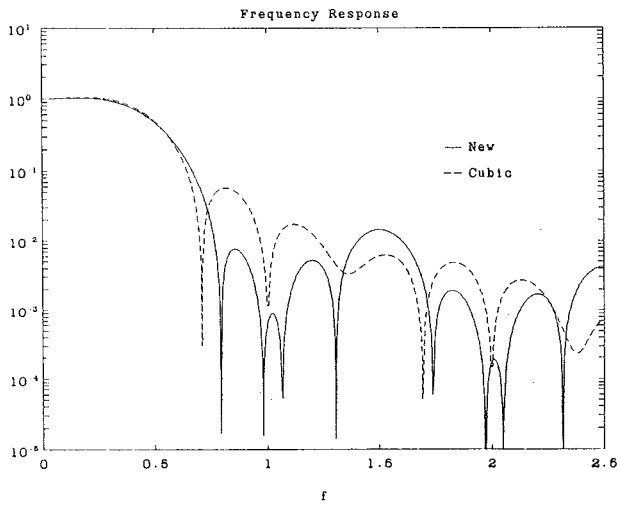

Figure 3: Spatial and frequency response characteristics of the optimal 4×4-point interpolator for aliased imagery corresponding to $\rho = 0.9$ and $\sigma^2 = 0$. The cubic convolution interpolator is shown for comparison.

Kernel			Error (DN)	
Type	ρ	size	RMS	Peak
New	0.9	2×2	4.9	24
Bilinear	–	2×2	5.1	26
New	0.9	4×4	2.5	12
Cubic	–	4×4	3.2	15
New	0.9	8×8	2.1	10
Hamming	–	8×8	1.8	8
New	0.9	16×16	2.1	10
Kaiser	–	16×16	1.4	7

Table 2: Resampling performance of kernels for aliased imagery.

Resampling Experiments

An experimental framework similar to that described earlier was employed in the evaluation of these resampling kernels, though only noise-free ($\sigma^2 = 0$) scenarios were considered this time. Table 2 indicates the resampling results using kernels corresponding to $\rho = 0.9$. (In fact, resampling performance was observed to be relatively independent of ρ.) Improvements in performance can be noted for the smaller sized resamplers—indeed, the 4×4-point resampler gives 22% less resampling error than cubic convolution.

Discussion

Despite the simplicity of the models employed in this work, some remarkably effective resampling kernels have been developed for use with remotely-sensed data.

The first family, based on an overly-optimistic model assuming no aliasing in the sensing process, yields kernels whose performance virtually indistinguishable from the best of the popular resamplers, particularly in the case of large kernels. However, the new kernels, though sinc-like in appearance, exhibit considerably less damping than traditional Kaiser-windowed interpolators. In noisy environments, the appropriate optimum kernels significantly outperform the traditional resamplers, optimally combining noise removal (smoothing) and interpolation. These kernels may be of use in some resampling scenarios.

The second family of kernels is based on an overly-pessimistic model which assumes that significant aliasing is introduced in the sensing process. These kernels are especially effective for low-order interpolation, such as in the case of 4×4-point resampling. Much of this gain is due to the fact that the false contrast enhancement of cubic convolution is avoided. Kernels of this family also have a damped-sinc appearance, though the degree of damping is more pronounced than is commonly introduced with, for example, typical Kaiser windows.

Note that while it may seem tempting to by-pass the autoregressive autocorrelation models $R_z(\cdot)$ of this work and estimate the required values directly from data, this approach has some inherent difficulties:

1. it is only possible to estimate *samples* of the autocorrelation from our sampled data;
2. the quality of the estimation may be poor if the σ^2 is large; and
3. *some* additional assumption about the data such as band-limiting must be made to enable interpolation of the autocorrelation. This effectively prohibits the incorporation of aliasing into the framework.

Nevertheless, for the noise-free, band-limited case, this approach is feasible and was considered, in fact, by Shlien [3]. However, while kernels adapted locally to the data can give excellent resampling error performance, the results can be misleading. After accounting for the additional computation inherent in the accumulation of statistics, one finds, in practice, that the same level of performance can be attained much more cheaply simply by using a larger sized resampling kernel.

In conclusion, therefore, we have described an apparently useful framework for the design of interpolators for remotely-sensed data. Future work ought to address the development of more refined models for both the imagery and the satellite-dependent sensing process.

References

[1] G. Oetken, T.W. Parks, and H.W. Schüssler, "New Results in the Design of Digital Interpolators," *IEEE Trans. Acoust., Speech, Signal Processing,* vol. ASSP-23, no. 3, pp. 301-309, June 1975.

[2] A.D. Polydoros and E.N. Protonotarios, "Digital Interpolation of Stochastic Signals," *IEEE Trans. Circuits and Systems,* vol. CAS-26, no. 11, pp. 916-922, Nov. 1979.

[3] S. Shlien, "Geometric Correction, Registration, and Resampling of Landsat Imagery," *Canadian J. Remote Sensing,* no. 5, pp.74-89, 1979.

[4] A.V. Oppenheim and R.W. Schafer, *Discrete-Time Signal Processing,* Englewood Cliffs, NJ : Prentice-Hall, 1989.